

**New Sterically-hindered o-Quinones Annelated with Metal-dithiolate: Regiospecificity in  
Oxidative Addition Reactions of Bifacial Ligand to the Pd and Pt Complexes**

*Konstantin A. Martyanov, Vladimir K. Cherkasov, Gleb A. Abakumov, Maxim A. Samsonov, Vera V. Khrizanforova, Yulia H. Budnikova and Viacheslav A. Kuropatov*

Table of Contents

X-ray crystallography	2
UV/Vis spectra	4
<sup>1</sup> H-NMR spectra	5
<sup>13</sup> C-NMR spectra	6
<sup>31</sup> P-NMR spectra	7
Cyclic voltammograms	8
IR spectra	9
X-band EPR spectra	10
Literature	12

### X-ray crystallography

The X-ray diffraction data were collected on a Bruker D8 Quest (for **2a**, **2b**) and Agilent Xcalibur E (for **3**) diffractometers (Mo K $\alpha$  radiation,  $\omega$ -scan technique,  $\lambda = 0.71073 \text{ \AA}$ ). The intensity data were integrated by SAINT<sup>[1]</sup> (for **2a**, **2b**) and CrysAlisPro<sup>[2]</sup> (for **3**) programs. SADABS<sup>[3]</sup> for **2a**, **2b** and SCALE3 ABSPACK<sup>[4]</sup> for **3** were used to perform area-detector scaling and absorption corrections. The structures were solved by dual-space<sup>[5]</sup> method and were refined on  $F^2$  using all reflections with the SHELXTL package<sup>[6]</sup>. All non-hydrogen atoms were refined anisotropically. H atoms were placed in calculated positions and refined in the “riding model”. The details of crystallographic, collection and refinement data for **2a**, **2b** and **3** are presented in Table SI1. CCDC-1446632 (**2a**), 1446633 (**2b**), 1446634 (**3**) contain the supplementary crystallographic data for this paper. These data can be obtained free of charge from the Cambridge Crystallographic Data Centre via [www.ccdc.cam.ac.uk/data\\_request/cif](http://www.ccdc.cam.ac.uk/data_request/cif).

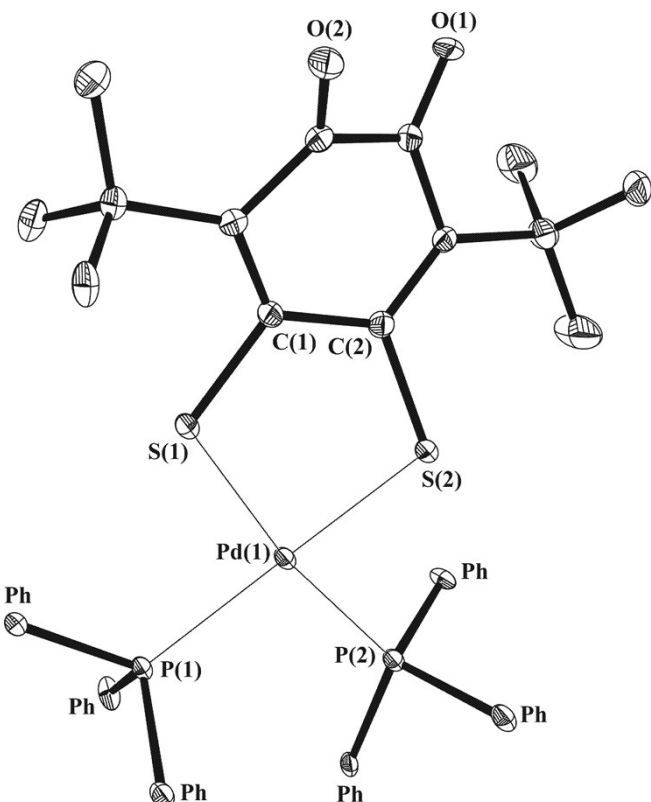


Figure SI1. An ORTEP plot of **2b**. Thermal ellipsoids are drawn at 50% probability.  
Hydrogen atoms are omitted and phenyl rings are marked “Ph” for clarity.

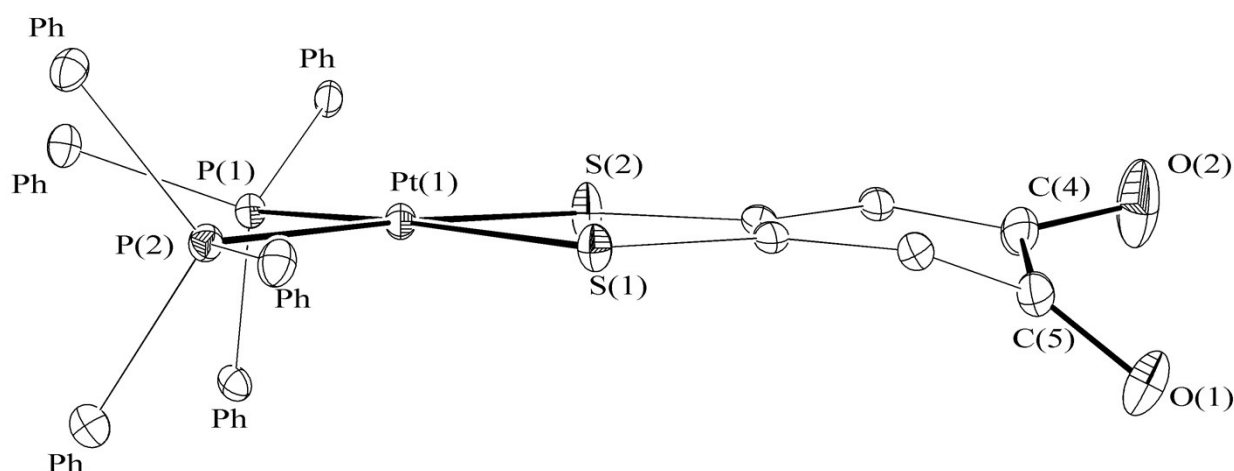


Figure SI2. An ORTEP plot of **3**, illustrating slightly distorted square planar surrounding of metal center and strong distortion in quinone ring. Thermal ellipsoids are drawn at 30% probability. Hydrogen atoms, tBu groups are omitted and phenyl rings are marked “Ph” for clarity.

Table SI1. Selected bond lengths, angles and torsions for **2** (M=Pd) and **3** (M=Pt)

	<b>2a</b>	<b>2b</b>	<b>3</b>
M(1) – P(1), Å	2.3411(5)	2.307(1)	2.3190(7)
M(1) – P(2), Å	2.3230(5)	2.322(1)	2.3078(7)
M(1) – S(1), Å	2.2707(5)	2.271(1)	2.2953(7)
M(1) – S(2), Å	2.2707(6)	2.287(1) [S(2)], 2.30(1) [S(2')] *	2.2971(7)
S(1) – M(1) – S(2), °	85.03(2)	85.58(4) [S(2)], 82.3(3) [S(2')] *	85.58(2)
P(1) – M(1) – P(2), °	98.71(2)	97.17(4)	97.93(2)
O(1)-C(5), Å	1.229(3) [O(1)], 1.289(8) [O(1')] *	1.229(5)	1.228(4)
O(2)-C(4), Å	1.224(3)	1.233(5)	1.231(4)
C(1)-C(6), Å	1.379(3)	1.368(6)	1.384(4)
C(1)-C(2), Å	1.493(3)	1.496(5)	1.512(4)
C(2)-C(3), Å	1.370(3)	1.370(5)	1.384(4)
C(3)-C(4), Å	1.453(3)	1.459(6)	1.455(4)
C(4)-C(5), Å	1.504(3)	1.527(6)	1.518(4)
C(5)-C(6), Å	1.454(3)	1.455(5)	1.467(4)
φ[O(1)-C(5)-C(4)-O(2)], °	39.6(3) [O(1)], 14.0(8) [O(1')] *	29.9(5)	37.3(4)

\* Two values are given owing to structural disordering on oxygen (**2a**) and sulfur (**2b**) atom

Table SI2. Crystallographic data and refinement parameters for **2** and **3**.

	2a	2b	3
Formula	C <sub>50</sub> H <sub>48</sub> O <sub>2</sub> P <sub>2</sub> PdS <sub>2</sub>	C <sub>52</sub> H <sub>52</sub> O <sub>2.5</sub> P <sub>2</sub> PdS <sub>2</sub>	C <sub>50</sub> H <sub>48</sub> O <sub>2</sub> P <sub>2</sub> PtS <sub>2</sub>
MW	913.34	949.39	1002.03
Crystal system	Monoclinic	Triclinic	Monoclinic
Space group	P <sub>2</sub> 1/c	P-1	P2 <sub>1</sub> /c
a, Å	9.7933(8)	10.760(2)	9.82880(10)
b, Å	27.530(2)	12.877(3)	27.6805(3)
c, Å	15.9433(13)	17.948(4)	16.0758(2)
α, °	90	95.401(3)	90
β, °	97.8730(10)	99.297(3)	98.0410(10)
γ, °	90	104.257(3)	90
V, Å <sup>3</sup>	4258.0(6)	2355.1(9)	4330.68(8)
Z,	4	2	4
ρ <sub>calcd.</sub> , g·cm <sup>-3</sup>	1.425	1.339	1.537
μ, mm <sup>-1</sup>	0.650	0.591	3.450
F(000)	1888	984	2016
Crystal dimension, mm	0.280 · 0.260 · 0.050	0.520 · 0.170 · 0.110	0.250 · 0.200 · 0.100
2θ range, °	2.424 – 26.000	3.031 – 27.000	3.042 – 25.999
Reflections measured	39437	18756	65836
Reflections with I ≥ 2σ(I)	7448	7872	7896
R <sub>1</sub> (all data)	0.0334	0.0785	0.0263
R <sub>1</sub> with I ≥ 2σ(I)	0.0280	0.0563	0.0233
wR <sub>2</sub> (all data)	0.0663	0.1448	0.0519
wR <sub>2</sub> with I ≥ 2σ(I)	0.0646	0.1361	0.0510
Goodness-of-fit on F <sup>2</sup>	1.061	1.050	1.121
Highest residue, e·Å <sup>-3</sup>	0.534	1.525	1.104
Lowest residue, e·Å <sup>-3</sup>	-0.332	-1.078	-1.152

### UV/Vis spectra

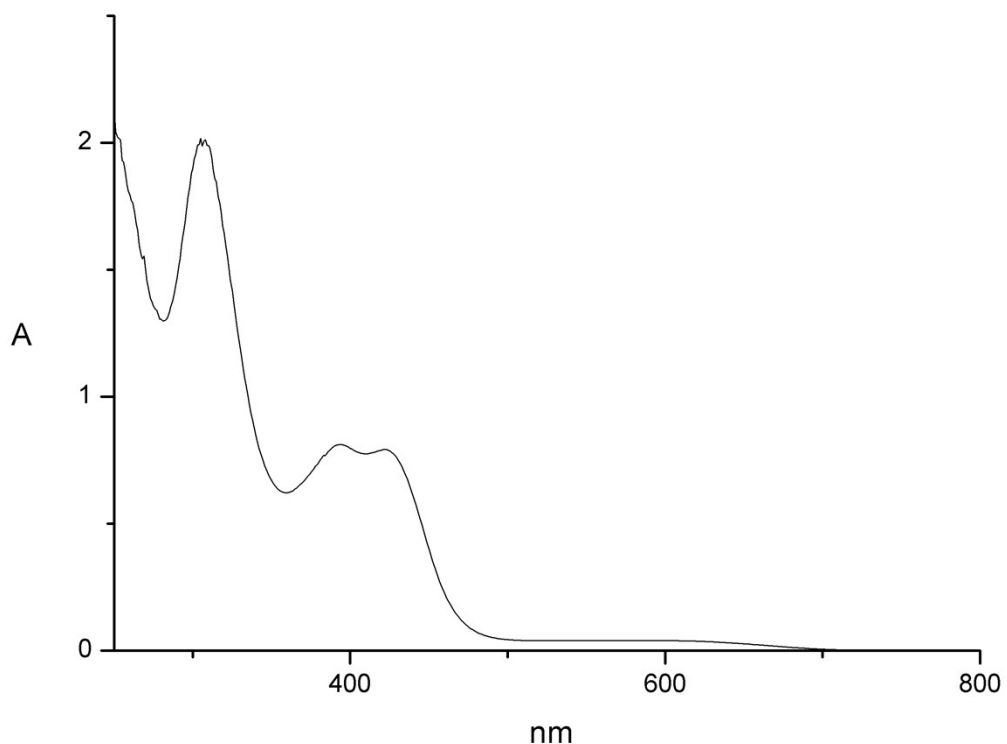


Figure SI3. UV/Vis spectrum of **2** in THF,  $c = 4.11 \cdot 10^{-5} \text{ mol} \cdot \text{L}^{-1}$ , 1.0 cm quartz cell;  $\epsilon = 520 \text{ M}^{-1} \text{cm}^{-1}$  ( $\lambda_{\max} = 588 \text{ nm}$ ),  $\epsilon = 19800 \text{ M}^{-1} \text{cm}^{-1}$  ( $\lambda_{\max} = 422 \text{ nm}$ ),  $\epsilon = 20200 \text{ M}^{-1} \text{cm}^{-1}$  ( $\lambda_{\max} = 398 \text{ nm}$ )

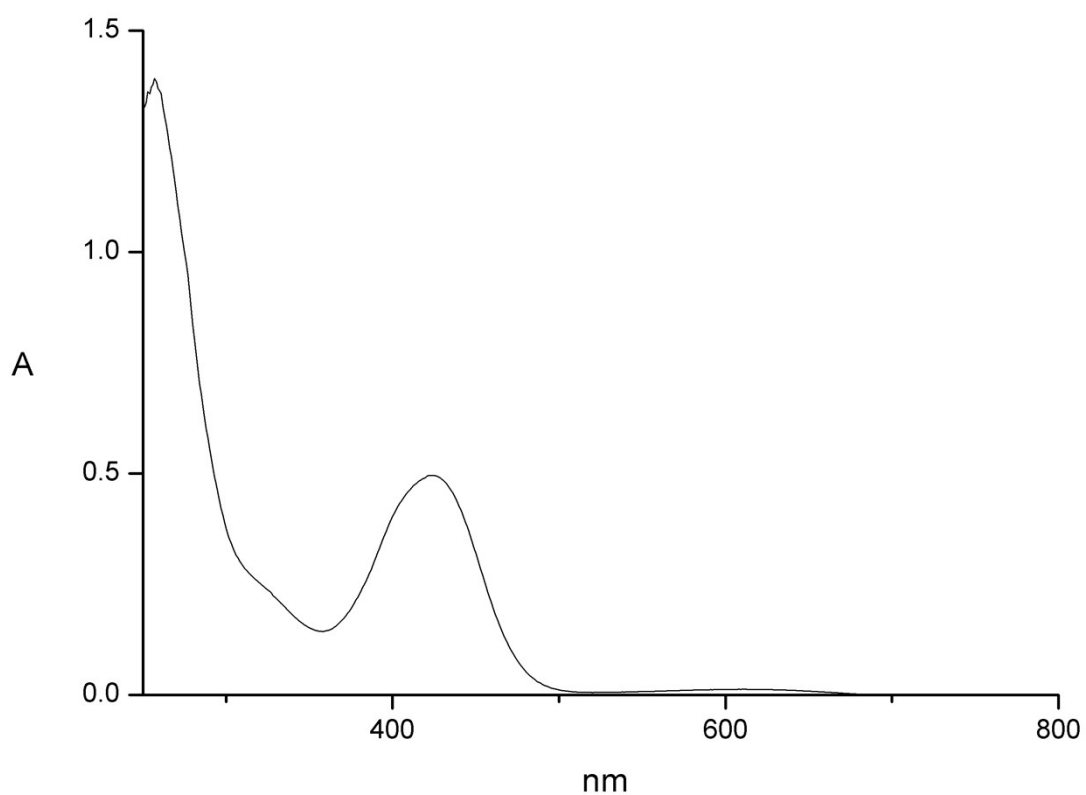


Figure SI4. UV/Vis spectrum of **3** in THF,  $c = 2.5 \cdot 10^{-5} \text{ mol} \cdot \text{L}^{-1}$ , 1.0 cm quartz cell;  $\epsilon = 580 \text{ M}^{-1} \text{cm}^{-1}$  ( $\lambda_{\max} = 611 \text{ nm}$ ),  $\epsilon = 19900 \text{ M}^{-1} \text{cm}^{-1}$  ( $\lambda_{\max} = 424 \text{ nm}$ )

### <sup>1</sup>H-NMR spectra

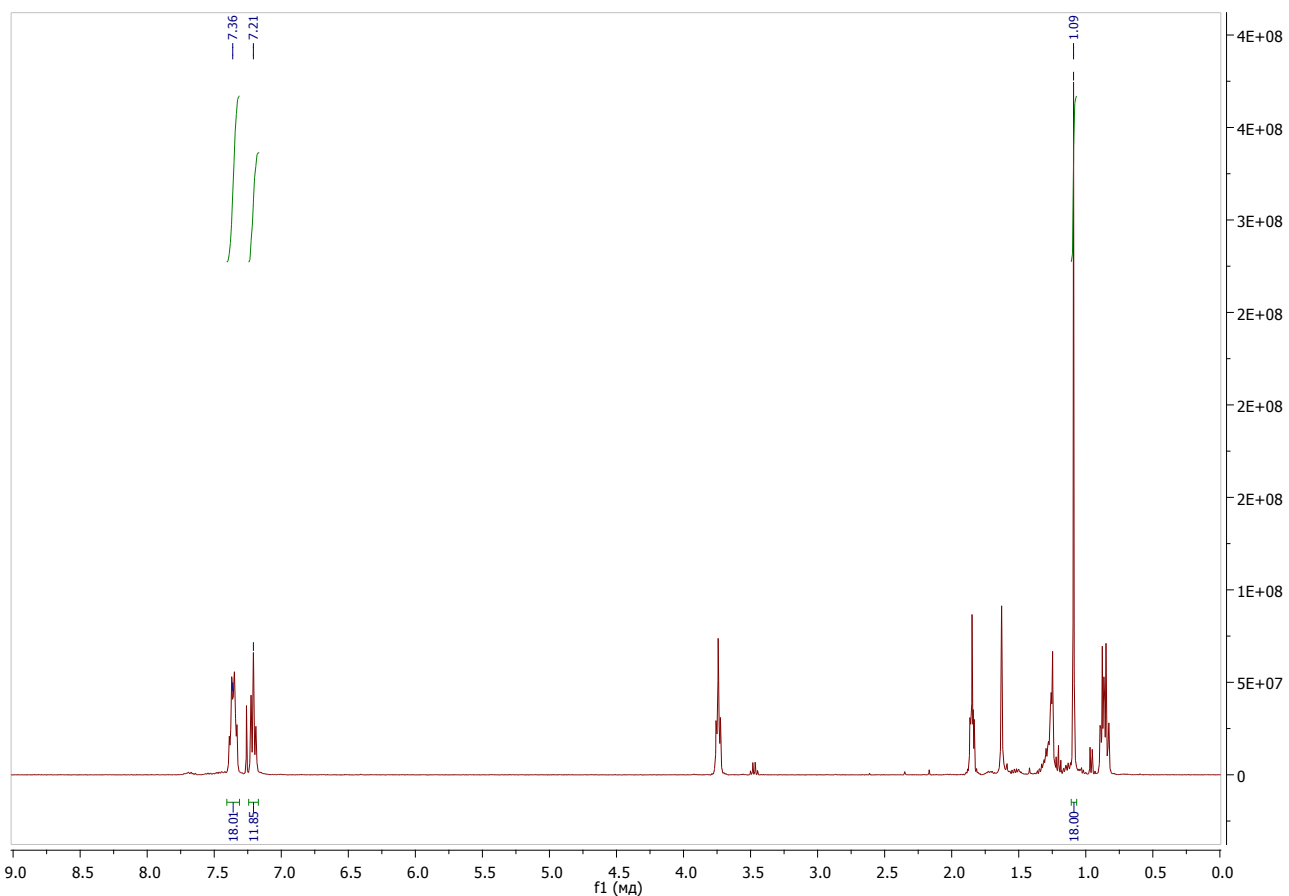


Figure SI5. <sup>1</sup>H NMR spectrum of **2** (400 MHz, CDCl<sub>3</sub>, 25°C)

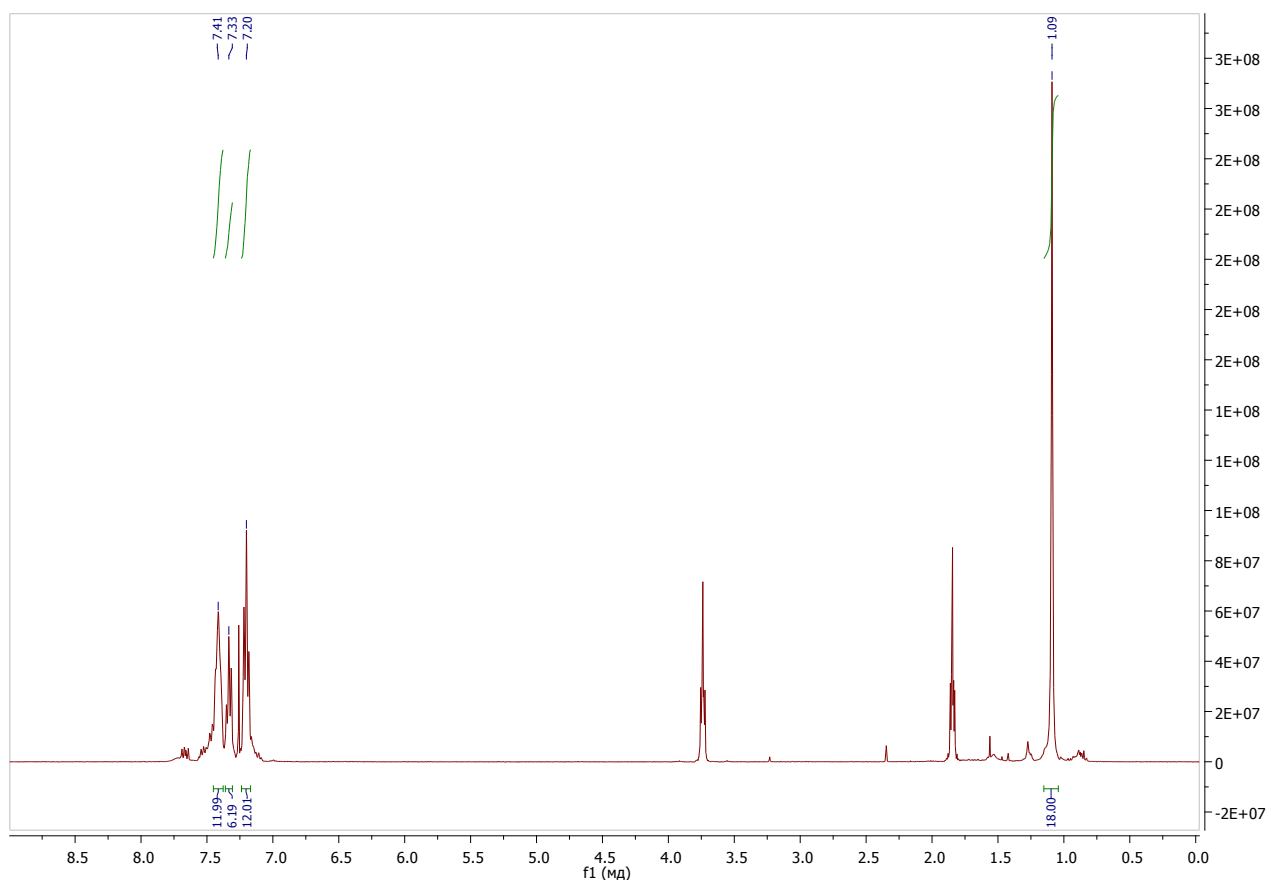


Figure SI6. <sup>1</sup>H NMR spectrum of **3** (400 MHz, CDCl<sub>3</sub>, 25°C)

### <sup>13</sup>C-NMR spectra

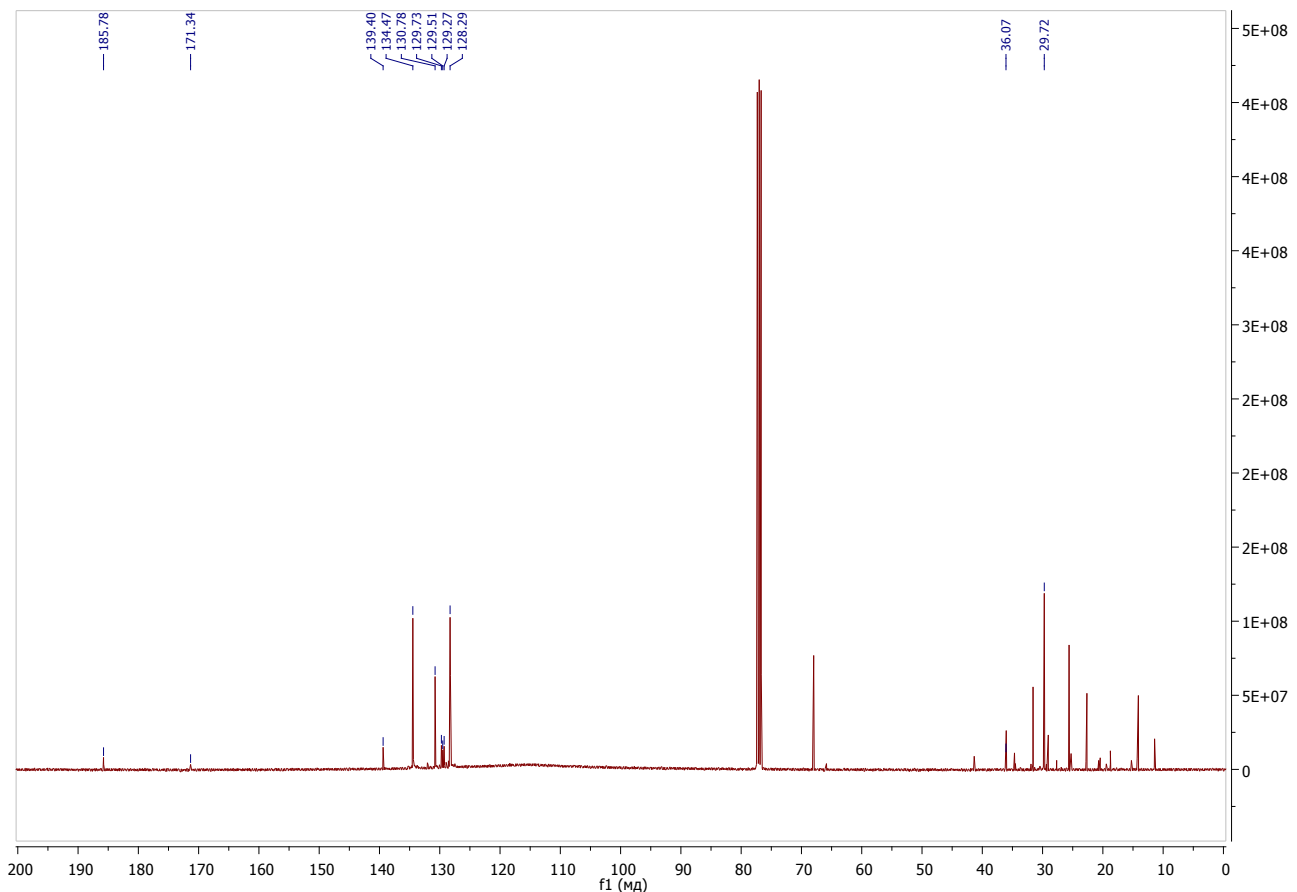


Figure SI7. <sup>13</sup>C NMR spectrum of **2** (100 MHz, CDCl<sub>3</sub>, 25°C)

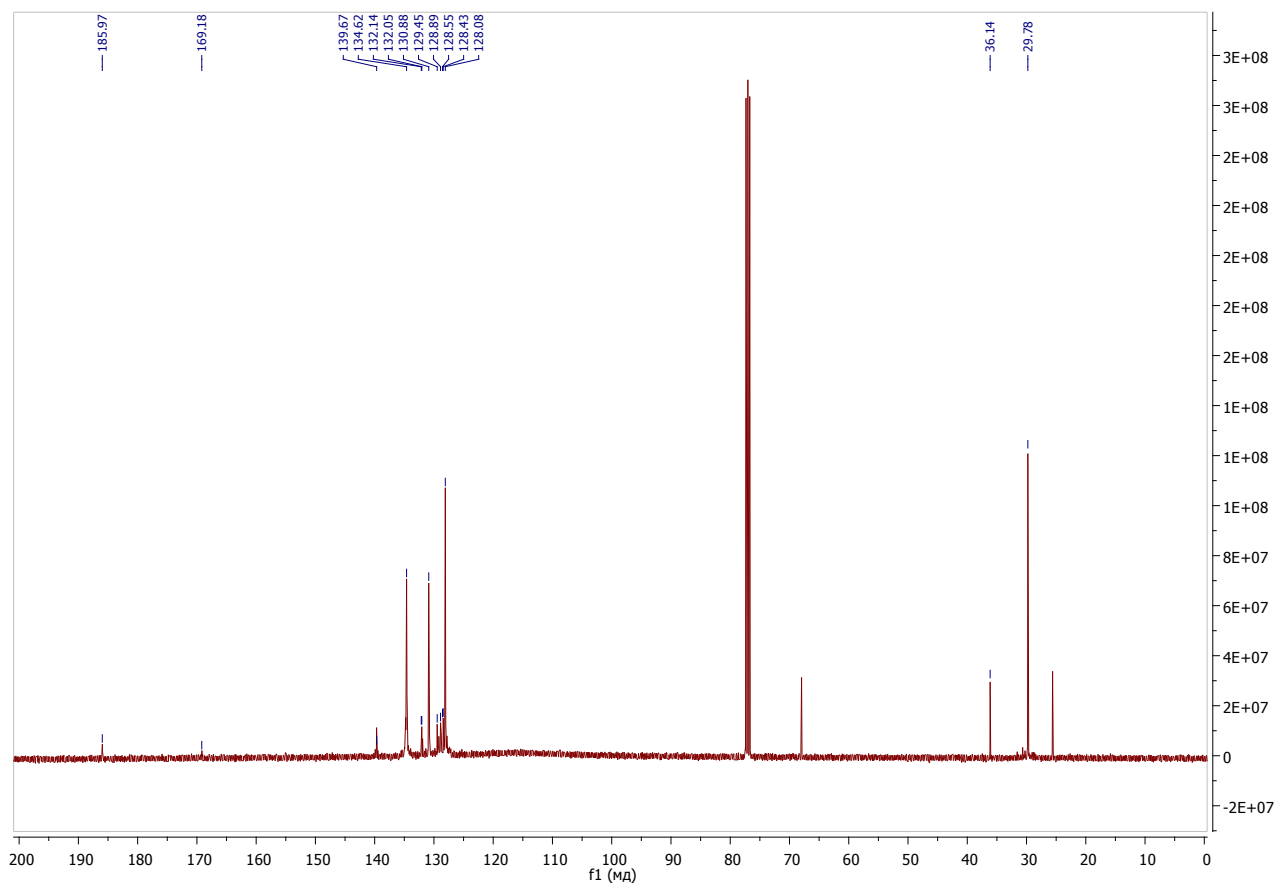


Figure SI8. <sup>13</sup>C NMR spectrum of **3** (100 MHz, CDCl<sub>3</sub>, 25°C)

### <sup>31</sup>P-NMR spectra

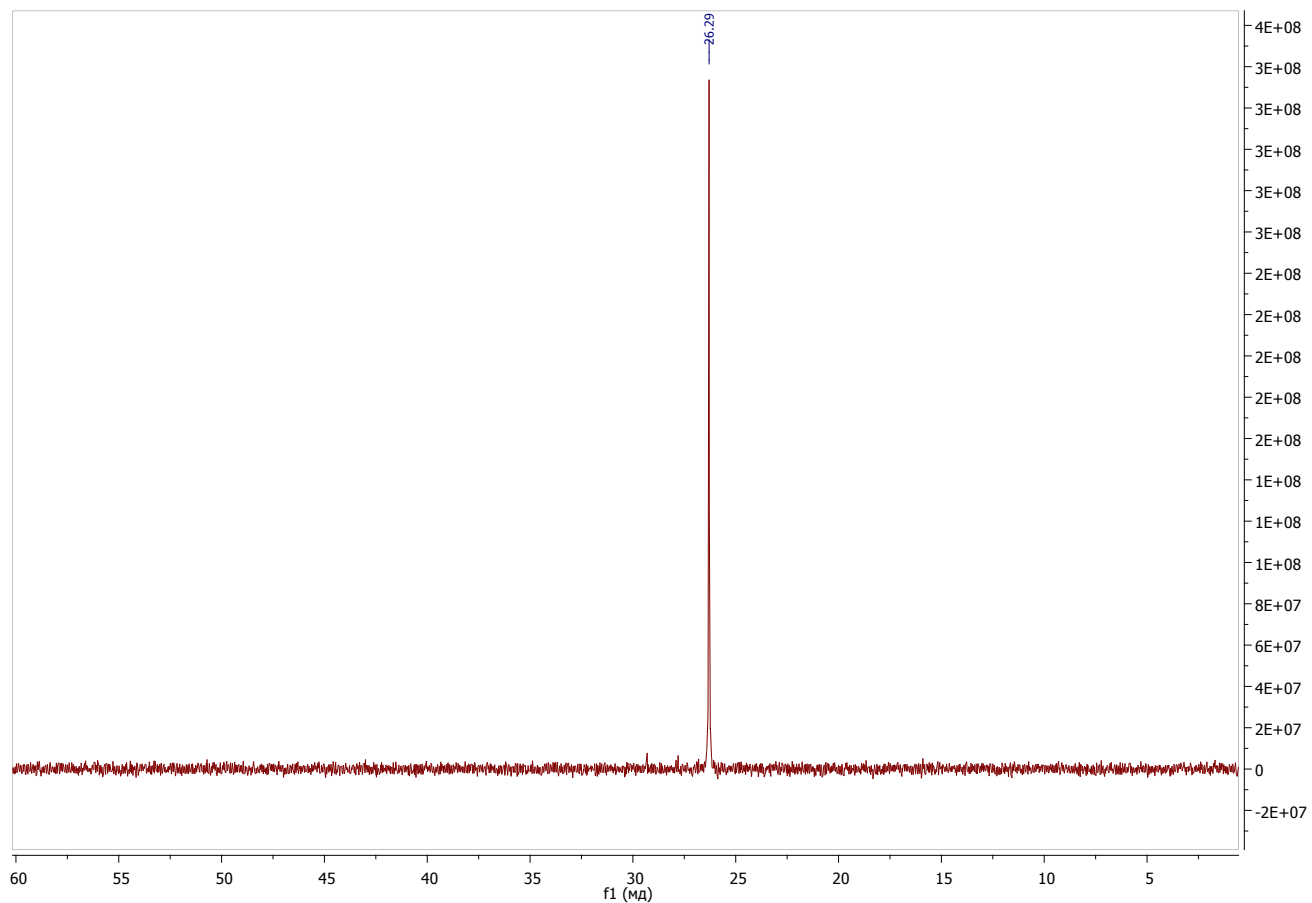


Figure SI9. <sup>31</sup>P NMR spectrum of **2** (161.97 MHz, CDCl<sub>3</sub>, 25°C)

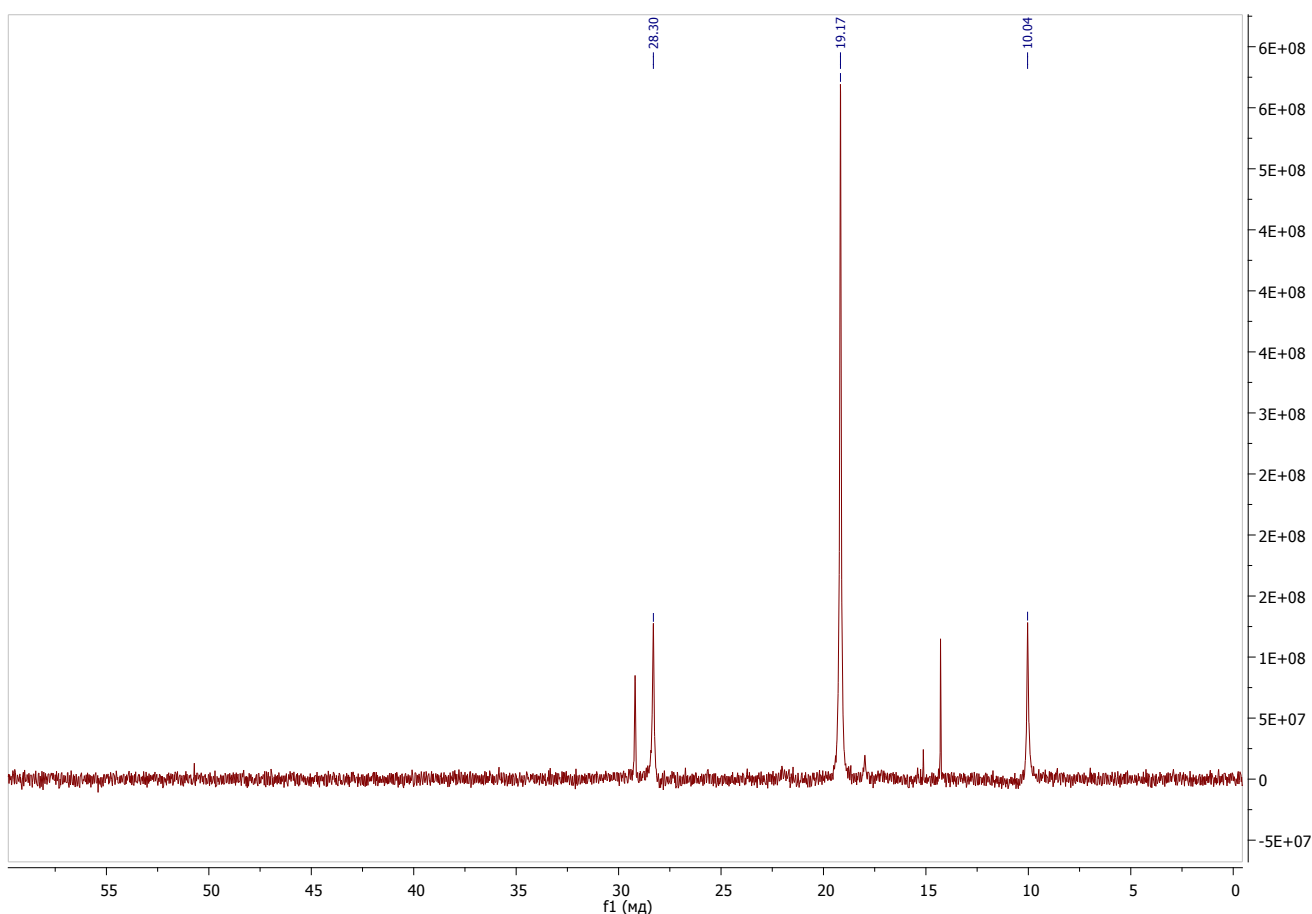


Figure SI10. <sup>31</sup>P NMR spectrum of **3** (161.97 MHz, CDCl<sub>3</sub>, 25°C)

### Cyclic voltammograms

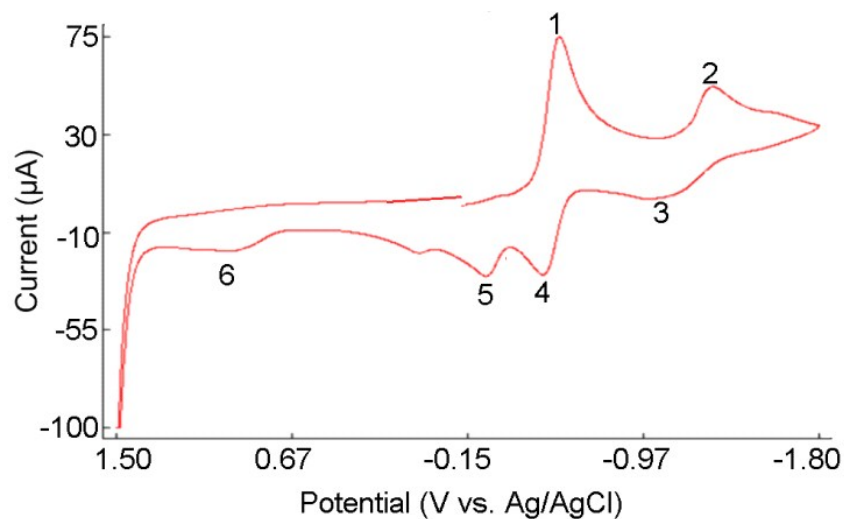


Figure SI11. Cyclic voltammogram of parent *o*-quinone **1** (DMF, vs Ag/AgCl)

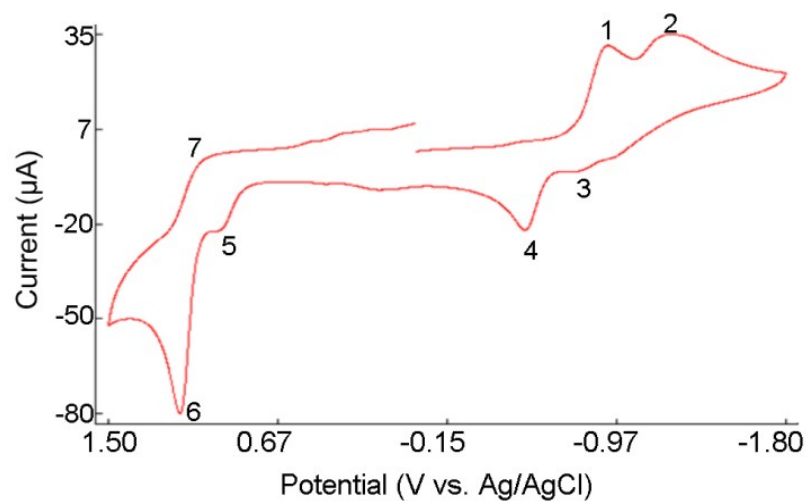


Figure SI12. Cyclic voltammogram of complex **2** (DMF, vs Ag/AgCl)

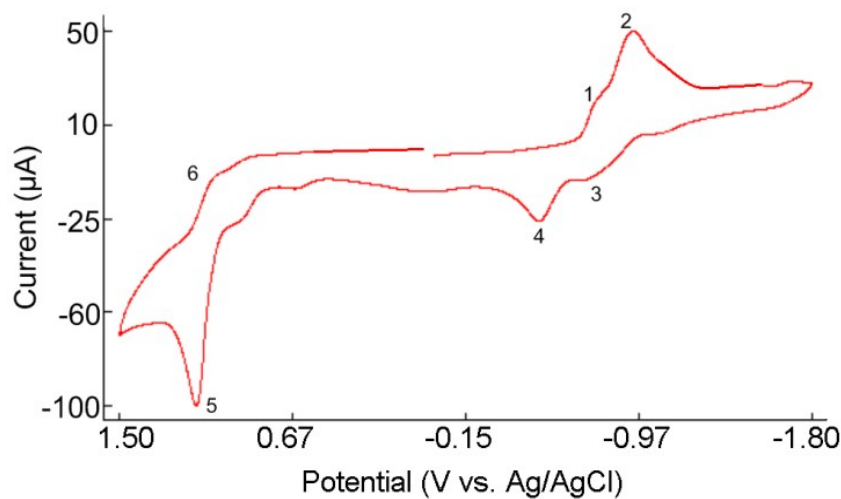


Figure SI13. Cyclic voltammogram of complex **3** (DMF, vs Ag/AgCl)

### IR spectra

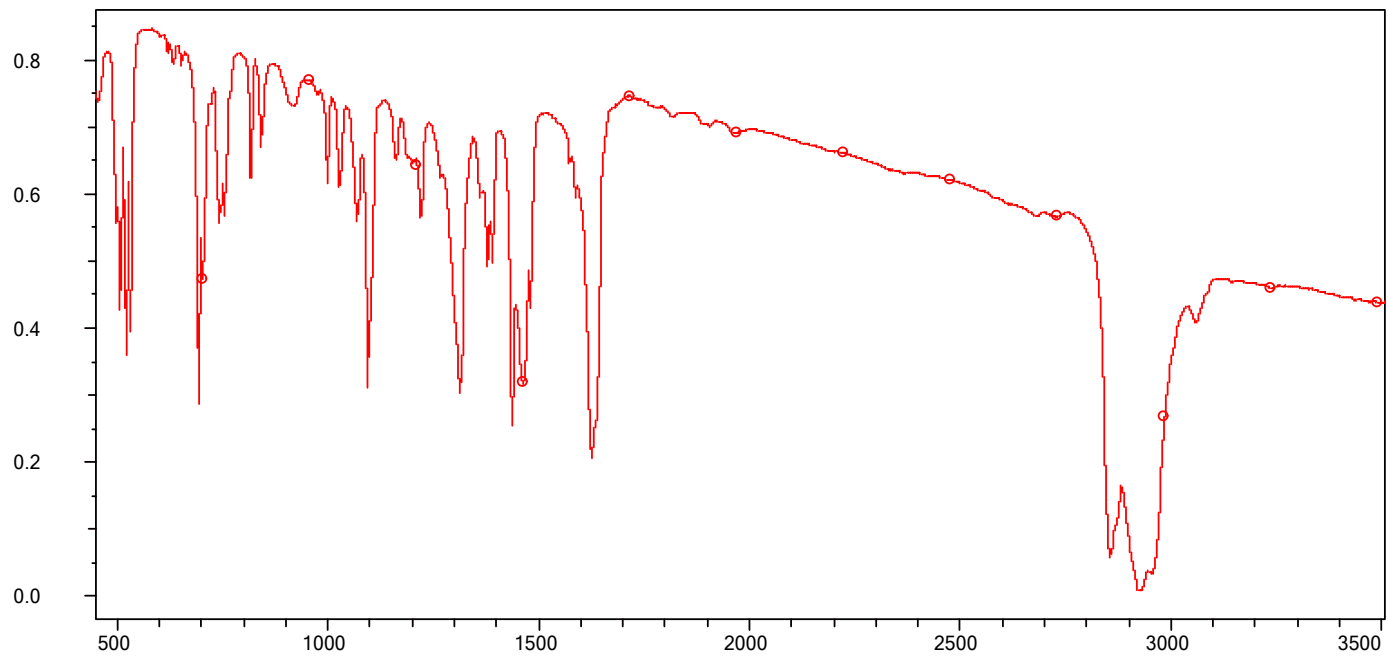


Figure SI14. IR spectrum of **2** in nujol

$\nu = 1624\text{s (C=O)}, 1435, 1307, 1216, 1189, 1159, 1091, 1026, 997, 914, 840, 813, 754, 692 \text{ cm}^{-1}$

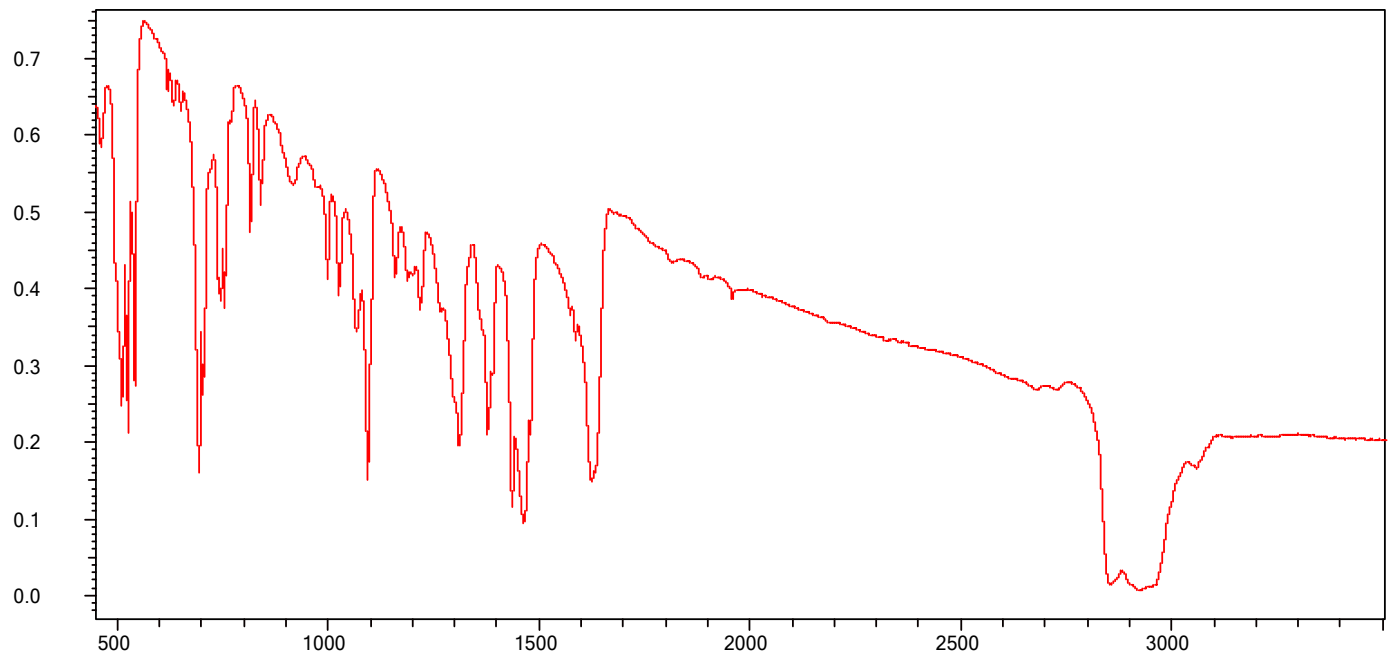
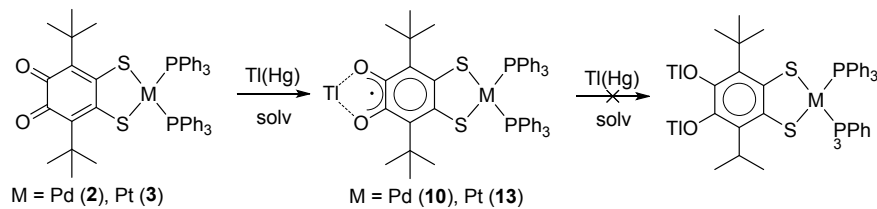


Figure SI15. IR spectrum of **3** in nujol

$\nu = 1624\text{s (C=O)}, 1438, 1313, 1217, 1163, 1096, 1067, 1029, 996, 912, 841, 816, 754, 741, 691 \text{ cm}^{-1}$

### X-band EPR spectra



Scheme SI11. Synthesis of dithiolate complexes **10** and **13** from **2** and **3**

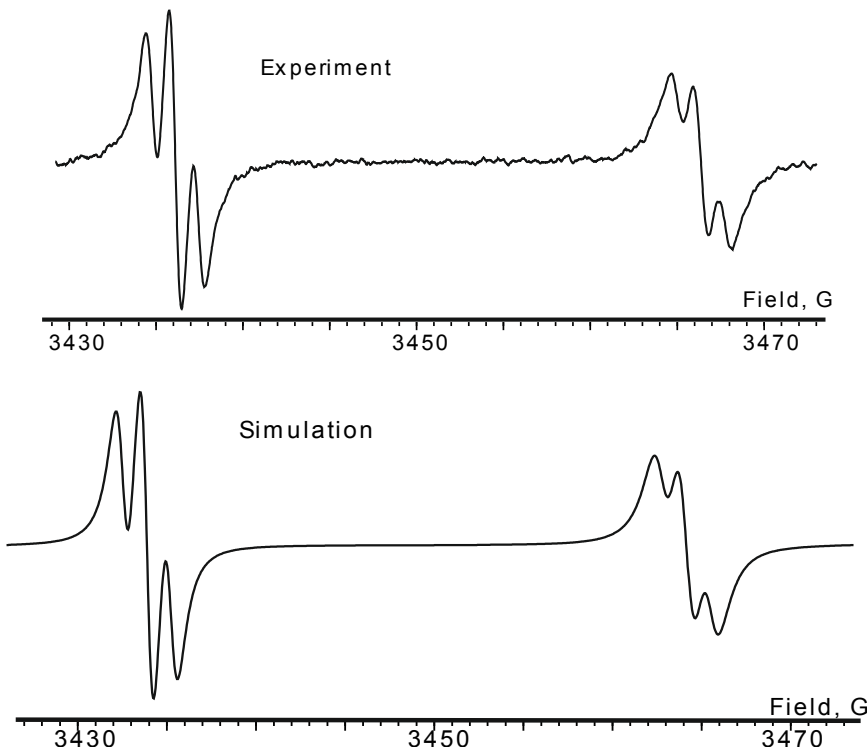


Figure SI16. Experimental (top) and simulated (bottom) X-band EPR spectra of **10** in THF, 298K.

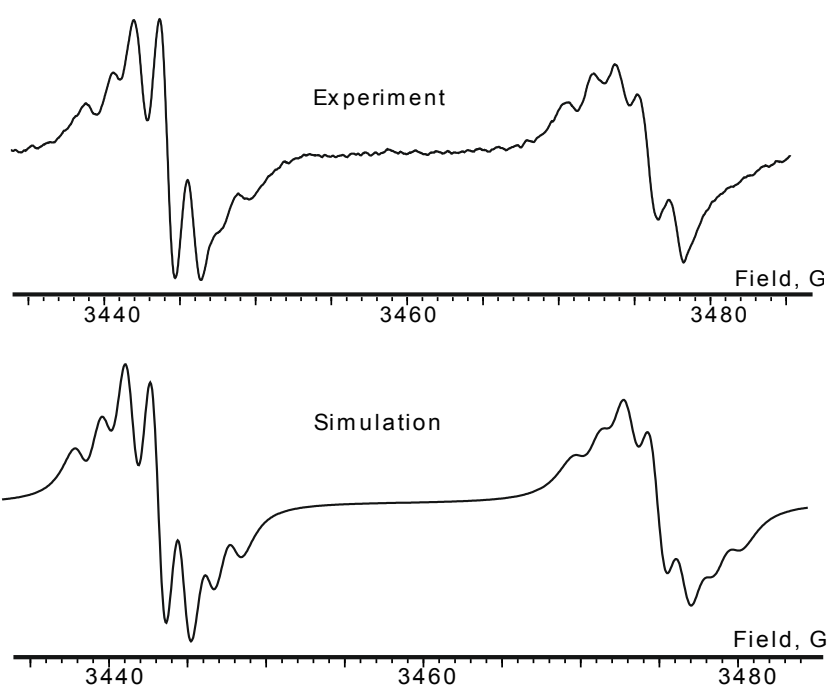


Figure SI17. Experimental (top) and simulated (bottom) X-band EPR spectra of **13** in THF, 298K.

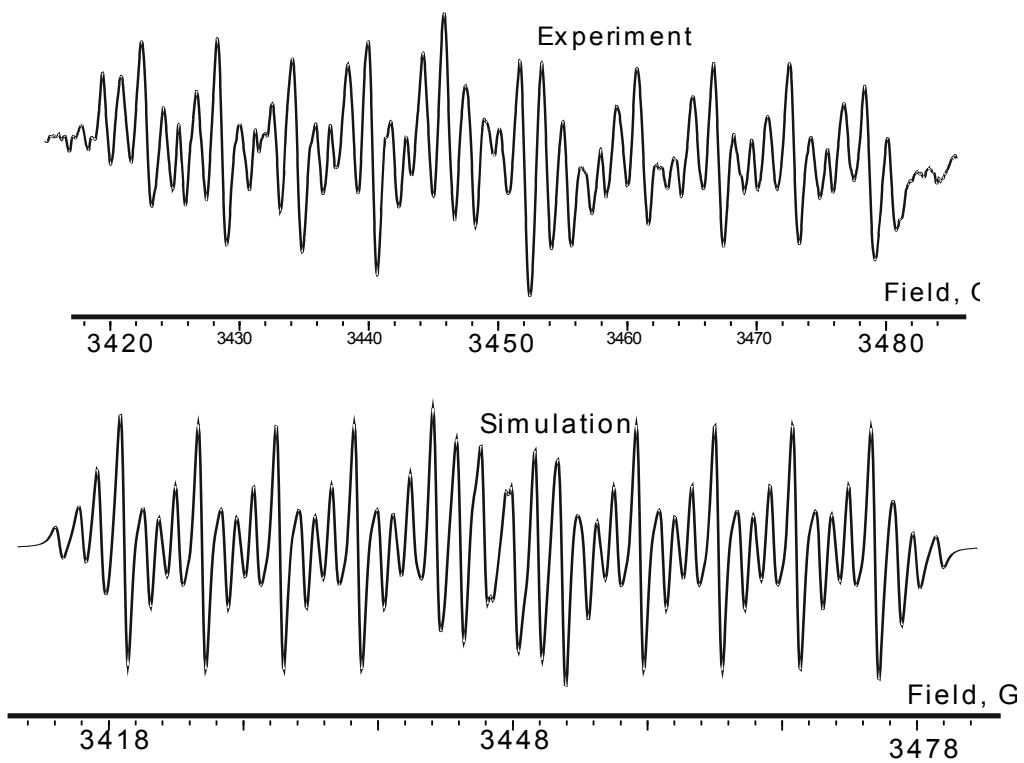


Figure SI18. Experimental (top) and simulated (bottom) X-band EPR spectra of **15** in THF, 298K.

## **Literature**

- [1] SAINT. Data Reduction and Correction Program. Version 8.27B. Bruker AXS Inc., Madison, Wisconsin, USA, 2012.
- [2] Data Collection. Reduction and Correction Program. CrysaliisPro – Software Package Agilent Technologies, 2012.
- [3] G.M. Sheldrick, SADABS-2012/1. Bruker/Siemens Area Detector Absorption Correction Program. Bruker AXS Inc., Madison, Wisconsin, USA, 2012.
- [4] SCALE3 ABSPACK: Empirical absorption correction, CrysaliisPro – Software Package Agilent Technologies, 2012.
- [5] G.M. Sheldrick, *Acta Cryst.* 2015, A71, 3-8.
- [6] G.M. Sheldrick, SHELXTL v. 6.14, Structure Determination Software Suite, Bruker AXS, Madison, Wisconsin, USA, 2003.